

The influence of critical behavior on the spin glass phase

Hemant Bokil

Abdus Salam ICTP, Strada Costiera 11, 34100 Trieste, Italy

Barbara Drossel

School of Physics and Astronomy, Raymond and Beverley Sackler Faculty of Exact Sciences, Tel Aviv University, Tel Aviv 69978, Israel

M. A. Moore

Department of Physics, University of Manchester, Manchester M13 9PL, U.K.

(November 20, 2018)

We have argued in recent papers that the Monte Carlo results for the equilibrium properties of the Edwards-Anderson spin glass in three dimensions, which had been interpreted earlier as providing evidence for replica symmetry breaking, can be explained quite simply within the droplet model once finite size effects and proximity to the critical point are taken into account. In this paper we show that similar considerations are sufficient to explain the Monte Carlo data in four dimensions. In particular, we study the Parisi overlap and the link overlap for the four-dimensional Ising spin glass in the Migdal-Kadanoff approximation. Similar to what is seen in three dimensions, we find that temperatures well below those studied in the Monte Carlo simulations have to be reached before the droplet model predictions become apparent. We also show that the double-peak structure of the link overlap distribution function is related to the difference between domain-wall excitations that cross the entire system and droplet excitations that are confined to a smaller region.

I. INTRODUCTION

Despite over two decades of work, the controversy concerning the nature of the ordered phase of short range Ising spin glasses continues. For a few years, Monte Carlo simulations appeared to be providing evidence for replica symmetry breaking (RSB) in these systems [1,2]. However, recent developments have cast doubt on this interpretation of the Monte Carlo data. In a series of papers on the Ising spin glass within the Migdal-Kadanoff approximation (MKA), we showed that the equilibrium Monte Carlo data in three dimensions that had been interpreted in the past as giving evidence for RSB can actually be interpreted quite easily within the droplet picture, with apparent RSB effects being attributed to a crossover between critical behavior and the asymptotic droplet-like behavior for small system sizes [3–6]. We also showed that system sizes well beyond the reach of current simulations would probably be required in order to unambiguously see droplet-like behavior. The finding that the critical-point effects can still be felt at temperatures lower than those accessible by Monte Carlo simulations is supported by the Monte Carlo simulations of Berg and Janke [7] who found critical scaling working reasonably well down to $T = 0.8T_c$ for system sizes upto $L = 8$ in three dimensions. The zero temperature study of Pallassini and Young [8] also suggests that the ground-state structure of three-dimensional Edwards-Anderson model is well described by droplet theory, though the existence of low energy excitations not included in the conventional

droplet theory remains an open question. Thus, while puzzles do remain, the weight of the evidence seems to be shifting towards a droplet-like description of the ordered phase in short range Ising spin glasses.

However, it is expected that critical point effects are less dominant in four dimensions than in three dimensions. Our aim in this paper is to quantify the extent of critical point effects in the low temperature phase of the four-dimensional Edwards-Anderson spin glass. We do this by providing results for the four-dimensional Ising spin glass in the MKA and compare these with existing Monte Carlo work. In particular, we study the Parisi overlap function and the link overlap function for system sizes up to $L = 16$ and temperatures as low as $T = 0.16T_c$. We find that for system sizes and temperatures comparable to those of the Monte Carlo simulations, the Parisi overlap distribution shows also in MKA the sample-to-sample fluctuations and the stationary behavior at small overlap values, that are normally attributed to RSB. It is only for larger system sizes (or for lower temperatures), that the asymptotic droplet-like behavior becomes apparent. For the link overlap, we find similar double-peaked curves as those found in Monte-Carlo simulations. This double peak structure is expected on quite general grounds independent of the nature of the low temperature phase. However, we show that two peaks in the link overlap in MKA occur because of a difference between domain-wall excitations (which cross the entire system) and droplet excitations (which do not cross the entire system). We argue that for small

system sizes, the effect of domain walls increases with increasing dimension, making it necessary to go very far below T_c to see the asymptotic droplet behavior.

This paper is organized as follows: in section II, we define the quantities discussed in this paper, and the droplet-model predictions for their behavior. In section III, we describe the MKA, and our numerical methods of evaluating the overlap distribution. In section IV, we present our numerical results for the Parisi overlap distribution, and compare to Monte-Carlo data. The following section studies the link overlap distribution. Finally, section VI contains the concluding remarks, including some on the effects of critical behavior on the dynamics in the spin glass phase. Again we suspect that arguments which have been advanced against the droplet picture on the basis of dynamical studies have failed to take into account the effects arising from proximity to the critical point.

II. DEFINITIONS AND SCALING LAWS

The Edwards-Anderson spin glass in the absence of an external magnetic field is defined by the Hamiltonian

$$H = - \sum_{\langle i,j \rangle} J_{ij} S_i S_j,$$

where the Ising spins can take the values ± 1 , and the nearest-neighbor couplings J_{ij} are independent from each other and Gaussian distributed with a standard deviation J .

It has proven useful to consider two identical copies (replicas) of the system, and to measure overlaps between them. This gives information about the structure of the low-temperature phase, in particular about the number of pure states. The quantities considered in this paper are the Parisi overlap function $P(q, L)$ and the link overlap function $P(q_l, L)$. They are defined by

$$P(q, L) = \left[\left\langle \delta \left(\sum_{\langle i,j \rangle} \frac{S_i^{(1)} S_i^{(2)} + S_j^{(1)} S_j^{(2)}}{2N_L} - q \right) \right\rangle \right], \quad (1)$$

and

$$P(q_l, L) = \left[\left\langle \delta \left(\sum_{\langle i,j \rangle} \frac{S_i^{(1)} S_i^{(2)} S_j^{(1)} S_j^{(2)}}{N_L} - q_l \right) \right\rangle \right]. \quad (2)$$

Here, the superscripts (1) and (2) denote the two replicas of the system, N_L is the number of bonds, and $\langle \dots \rangle$ and $[\dots]$ denote the thermodynamic and disorder average respectively. We use $P(q, L)$ and $P(q_l, L)$ to denote the overlap functions for a finite system of size L , reserving the more standard notation $P(q)$ and $P(q_l)$ for the limit $\lim_{L \rightarrow \infty} P(q, L)$ and $\lim_{L \rightarrow \infty} P(q_l, L)$.

In the mean-field RSB picture, $P(q)$ is nonzero in the spin glass phase in the entire interval $[-q_{EA}, q_{EA}]$, while

it is composed only of two delta functions at $\pm q_{EA}$ in the droplet picture. Similarly, $P(q_l)$ is nonzero over a finite interval $[q_l^{min}, q_l^{max}]$ in mean-field theory, while it is a delta-function within the droplet picture.

Much of the evidence for RSB for three- and four-dimensional systems comes from observing a stationary $P(q = 0, L)$ for system sizes that are generally smaller than 20 in 3D and smaller than 10 in 4D, and at temperatures of the order of $0.7T_c$. However, even within the droplet picture one expects to see a stationary $P(q = 0, L)$ for a certain range of system sizes and temperatures. The reason is that at T_c the overlap distribution $P(q, L)$ obeys the scaling law

$$P(q, L) = L^{\beta/\nu} \tilde{P}(q L^{\beta/\nu}), \quad (3)$$

β being the order parameter critical exponent, and ν the correlation length exponent. Above the lower critical dimension (which is smaller than 3), β/ν is positive, leading to an increase $P(q = 0, L)$ as a function of L (at $T = T_c$). On the other hand, for $T \ll T_c$, the droplet model predicts a decay

$$P(q = 0, L) \sim 1/L^\theta$$

on length scales larger than the (temperature-dependent) correlation length ξ , θ being the scaling exponent of the coupling strength J . A few words are in order here on what we mean by the correlation length. In the spin glass phase, all correlation functions fall off as a power law at large distances. However, within the droplet model, this is true only asymptotically, and the general form of the correlation function for two spins a distance r apart, at a temperature $T \leq T_c$, is $\sim r^{-\theta} f(r/\xi)$ where k_B is the Boltzmann constant and f is a scaling function. Thus, for $r \leq \xi$ there are corrections to the algebraic long-distance behavior and the above expression defines the temperature-dependent correlation length. Note that for $T \rightarrow T_c$ this correlation length is expected to diverge with the exponent ν .

Thus, for temperatures not too far below T_c , one can expect an almost stationary $P(q = 0, L)$ for a certain range of system sizes. In three dimensions both $\beta/\nu \simeq 0.3$ [7] and $\theta \simeq 0.17$ [9] are rather small, this apparent stationarity may persist over a considerable range of system sizes L . However, in four dimensions, $\beta/\nu \simeq 0.85$ [10] and $\theta \simeq 0.65$ [11] and one would expect the crossover region to be smaller. In the present paper we shall investigate these crossover effects in four dimensions by studying $P(q, L)$ for the Edwards-Anderson spin glass within the MKA. It turns out that they are surprisingly persistent even at low temperatures, due to the presence of domain walls.

Monte-Carlo simulations of the link overlap distribution show a nontrivial shape with shoulders or even a double peak, which seems to be incompatible with the

droplet picture, where the distribution should tend towards a delta-function. For sufficiently low temperatures and large length scales, the droplet picture predicts that the width of the link overlap distribution scales as [6]

$$\Delta q_l \sim \sqrt{kT} L^{d_s - d - \theta/2},$$

where d_s is the fractal dimension of a domain wall. Below, we will show that the nontrivial shape and the double peak reported from Monte-Carlo simulations are also found in MKA in four dimensions, and we will present strong evidence that it is due to the different nature of droplet and domain wall excitations. As the weight of domain walls becomes negligible in the thermodynamic limit, the droplet picture is regained on large scales.

III. MIGDAL-KADANOFF APPROXIMATION

The Migdal-Kadanoff approximation (MKA) is a real-space renormalization group that gives approximate recursion relations for the various coupling constants. Evaluating a thermodynamic quantity in MKA in d dimensions is equivalent to evaluating it on an hierarchical lattice that is constructed iteratively by replacing each bond by 2^d bonds, as indicated in Fig. 1. The total number of bonds after I iterations is 2^{dI} . $I = 1$, the smallest non-trivial system that can be studied, corresponds to a system linear dimension $L = 2$, $I = 2$ corresponds to $L = 4$, $I = 3$ corresponds to $L = 8$ and so on. Note that the number of bonds on hierarchical lattice after I iterations is the same as the number of sites of a d -dimensional lattice of size $L = 2^I$. Thermodynamic quantities are then evaluated iteratively by tracing over the spins on the highest level of the hierarchy, until the lowest level is reached and the trace over the remaining two spins is calculated [12]. This procedure generates new effective couplings, which have to be included in the recursion relations.

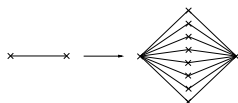


FIG. 1. Construction of a hierarchical lattice.

In [13], it was proved that in the limit of infinitely many dimensions (and in an expansion away from infinite dimensions) the MKA reproduces the results of the droplet picture.

As was discussed in [3], the calculation of $P(q, L)$ is made easier by first calculating its Fourier transform $F(y, L)$, which is given by

$$F(y, L) = \left[\left\langle \exp \left[iy \sum_{\langle ij \rangle} \frac{(S_i^{(1)} S_i^{(2)} + S_j^{(1)} S_j^{(2)})}{2N_L} \right] \right\rangle \right]. \quad (4)$$

The recursion relations for $F(y, L)$ involve two- and four-spin terms, and can easily be evaluated numerically because all terms are now in an exponential. Having calculated $F(y)$ one can then invert the Fourier transform to get $P(q, L)$.

Similarly, $P(q, L)$ is calculated by first evaluating

$$F(y_l, L) = \left[\left\langle \exp \left[iy_l \sum_{\langle ij \rangle} \frac{(S_i^{(1)} S_i^{(2)} S_j^{(1)} S_j^{(2)})}{N_L} \right] \right\rangle \right]. \quad (5)$$

Before presenting our numerical results for the Parisi overlap and the link overlap, let us discuss the flow of the coupling constant J in the low-temperature phase, as obtained in MKA. In order to obtain this flow, we iterated the MKA recursion relation on a set of 10^6 bonds. At each iteration, each of the new set of 10^6 bonds was generated by randomly choosing 16 bonds from the old set and taking the trace over the inner spins (with a bond arrangement as in Fig. 1). Figure 2 shows J/T as function of L for different initial values of the coupling strength. The critical point is at $T_c \simeq 2.1J$. The first curve begins at $J/T = 0.5$, which is close to the critical point, and it reaches the low-temperature behavior only at lengths around 1000. For an initial $J/T = 0.7$, the asymptotic slope is already reached at L around 40, and for $J/T = 3.0$, which corresponds to $T \simeq 0.16T_c$ the entire curve shows the asymptotic slope. The asymptotic slope is identical to the above-mentioned exponent θ and has the value $\theta \simeq 0.75$. In contrast to $d = 3$ [6], we did not succeed in fitting the crossover regime by doing an expansion around the zero-temperature fixed point. The reason is that dimension 4 is too far above the lower critical dimension, such that the critical temperature is not small.

Note that for each temperature the length scale beyond which the flows of the coupling constants show the asymptotic behavior yields one estimate for the correlation length mentioned above. We have considered the flow to be in the asymptotic regime when its slope was within 90% of its asymptotic value. However, this estimate is specific to the flows of the coupling constant, and other quantities may show their asymptotic behavior later. In fact, as we shall see below, the convergence of the overlap distributions is much slower than that of the couplings, and we will have to give reasons for this.

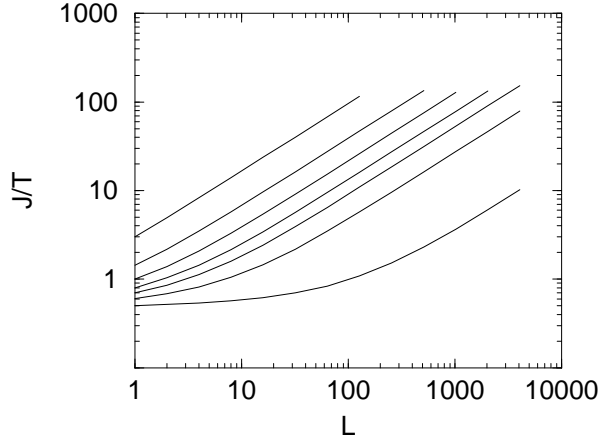


FIG. 2. Flow of the coupling strength J in MKA. The curves correspond to $T/T_c = 0.96, 0.8, 0.68, 0.6, 0.48, 0.33, 0.16$ (from bottom to top). The correlation lengths, where the slope has reached 90% of the asymptotic slope, are 960, 47, 24, 15, 8, 3, 1.

IV. THE PARISI OVERLAP

We now discuss our results for the Parisi overlap. First, let us briefly describe the critical behavior. Fig. 3 shows a scaling plot for $P(q, L)$ for $L = 4, 8, 16$ at $T = T_c \simeq 2.1J$. We find a good data collapse if we use the value $\beta/\nu = 0.64$, thus confirming the finite-size scaling ansatz Eq. 3.

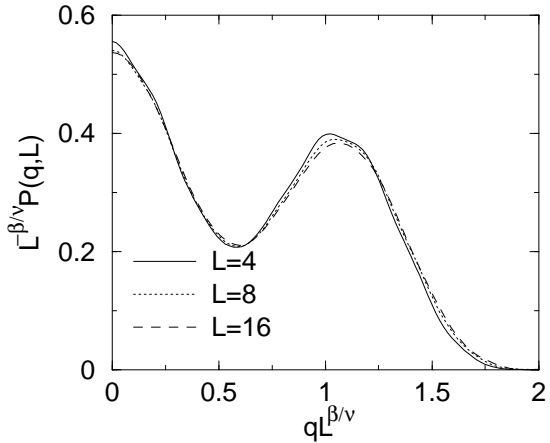


FIG. 3. Scaling collapse of $P(q, L)$ at $T = T_c$, with $\beta/\nu \simeq 0.64$. As $P(q, L) = P(-q, L)$, only the part $q \geq 0$ is shown. For each system size, we averaged over at least 5000 samples.

We next move on to the low-temperature phase. In Fig. 4 we show $P(q, L)$ at $T = 0.5T_c$ and $L = 8$ for three different samples.

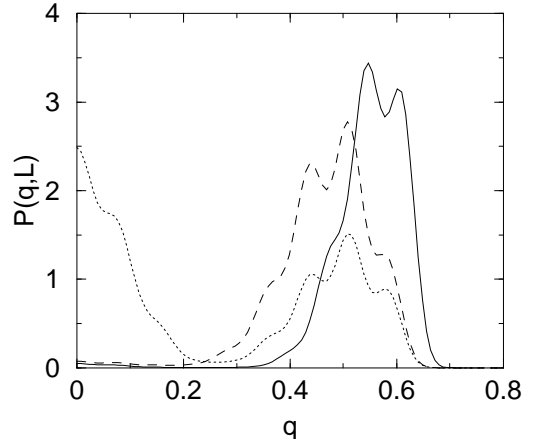


FIG. 4. $P(q, L)$ for three different samples at $T = 0.5T_c$ and $L = 8$.

As one can see there are substantial differences between the samples. This sensitivity to samples for system sizes around 10 is in [10] interpreted as evidence for RSB. In our case, where we know that the droplet model is exact, it has to be considered a finite size effect. Note that we have not chosen the three samples in any particular manner. By comparing to the curves obtained for $L = 16$ (not shown), we can even see the trend to an increasing number of peaks, just as in [10]. Thus, one feature commonly associated with RSB is certainly present in within the MKA for temperatures and system sizes comparable to those studied in simulations.

Let us now focus on the behavior of $P(q = 0, L)$ for different system sizes and temperatures. But before exhibiting our own data, we discuss the Monte Carlo data of Reger, Bhatt and Young [1] who were the first to study $P(q = 0, L)$ for the Edwards-Anderson spin glass. They studied system sizes $L = 2, 3, 4, 5, 6$ at temperatures down to $T = 0.68T_c$. At $T = T_c$ they found the expected critical scaling, $P(q = 0) \simeq L^{\beta/\nu}$ with $\beta/\nu \simeq 0.75$. Then, as the temperature was lowered, the curves for $P(q = 0)$ as a function of L showed a downward curvature for the largest system sizes, which they interpreted as the beginning of the crossover between critical behavior and the low temperature behavior. At $T = 0.8T_c$, $P(q = 0)$ seemed to be roughly constant or decreasing slowly. However, the striking part of their data was that at $T = 0.68T_c$ they found that $P(q = 0, L)$ initially decreased as a function of system size for $L = 2, 3, 4$ and then saturated for $L = 4, 5, 6$. They interpreted this as suggestive of RSB. They admitted however that other explanations are possible.

The most recent Monte-Carlo simulation data for the 4d Ising spin glass are those in [10]. These authors focus on $T \simeq 0.6T_c$, and they find an essentially stationary $P(q = 0, L)$ for system sizes up to the largest simulated size $L = 10$. They argue, that stationarity over such a large range of L values is most naturally interpreted as

evidence for RSB. However, as can be seen from Fig. 3, the correlation length is of the order of 16 for these temperatures and therefore comparable to the system size.

In Fig.5, we show the MKA data for $P(q = 0, L)$. We have calculated $P(q = 0, L)$ for system sizes $L = 4, 8, 16$ at temperatures $T = T_c$, $0.68T_c$, $0.33T_c$, and $0.16T_c$. At $T = T_c$, $P(q = 0, L)$ grows as $L^{\beta/\nu}$ with $\beta/\nu \simeq 0.64$, in agreement with Fig.3. At $T = 0.68T_c$ (the lowest temperature studied in [1], and not far from the lowest temperature studied by [10]), we do not see a clear decrease even for $L = 16$. The curve for $P(q = 0)$ looks more or less flat, though one could say that there is slight increase between $L = 4$ and $L = 8$ and a slight decrease between $L = 8$ and $L = 16$. This flat behavior is similar to what was found in [1] and [10]. The deviation of the $L = 2$ and $L = 3$ data from the flat curve in [1] can probably be ascribed to artifacts at very small system sizes, which are also found elsewhere [14]. For lower temperatures, where the correlation length is smaller than the system size, there is a clear decrease of $P(q = 0)$ although the decrease is not asymptotic even at a temperatures as low as $T_c/6$.

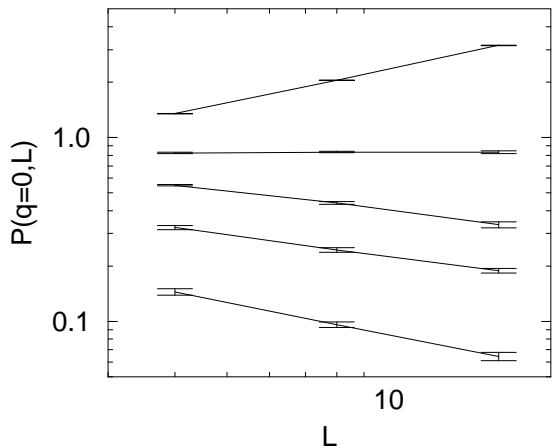


FIG. 5. $P(q = 0, L)$ at $T = T_c$, $0.68T_c$, $0.5T_c$, $0.33T_c$, $0.16T_c$ for $L=4,8,16$. The error bars indicate the standard deviation of the values. All data were obtained by averaging at least over 5000 samples.

We conclude that the observed stationarity of $P(q = 0, L)$ in Monte-Carlo data is due to the effects of a finite system size and finite temperature. Similarly, Monte-Carlo simulations at $T \simeq 0.5T_c$ and at system sizes around 10, should be able to show the negative slope in $P(q = 0, L)$. In the not too far future, it should become possible to perform these simulations.

The fact that $P(q = 0, L)$ does not show asymptotic behavior even at $T = T_c/6$ for the system sizes that we have studied, is surprising, and is different from our findings in $d = 3$ [3]. That $P(q = 0, L)$ converges slower towards the asymptotic behavior than the flow of the coupling constant (see Fig. 2), can be understood in the

following way: A Parisi overlap value close to zero can be generated by a domain wall excitation. For large system sizes and low temperatures, such an excitation occurs with significant weight only in those samples where a domain wall excitation costs little energy. These are exactly the samples with a small renormalized coupling constant at system size L . As the width of the probability distribution function of the couplings increases with L^θ , the probability for obtaining a small renormalized coupling decreases as $L^{-\theta}$. This is the argument that predicts that $P(q = 0, L) \sim L^{-\theta}$. However, for smaller system sizes and higher temperatures, there are corrections to this argument. Thus, even samples with a renormalized coupling that is not small can contribute to $P(q = 0, L)$ by means of large or multiple droplet excitations, or of thermally activated domain walls. For this reason, $P(q = 0, L)$ can be expected to converge towards asymptopia slower than the coupling constant itself. Furthermore, as we shall see in the next section, the superposition of domain wall excitations and droplet excitations leads to deviations from simple scaling, which may further slow down the convergence towards asymptotic scaling behavior.

V. THE LINK OVERLAP

The link overlap gives additional information about the spin glass phase that is not readily seen in the Parisi overlap. The main qualitative differences between the Parisi overlap and the link overlap are (i) that flipping all spins in one of the two replicas changes the sign of q but leaves q_l invariant, and (ii) that flipping a droplet of finite size in one of the two replicas changes q by an amount proportional to the volume of the droplet, and q_l by an amount proportional to the surface of the droplet. Thus, the link overlap contains information about the surface area of excitations.

First, let us study $P(q_l, L)$ as function of temperature, for a given system size $L = 4$. Fig. 6 shows our curves for $T = 0.8T_c$, $0.67T_c$, $0.56T_c$, $0.48T_c$, and $0.33T_c$. They appear to result from the superposition of two different peaks, with their distance increasing with decreasing temperature, and the weight shifting from the left peak to the right peak.

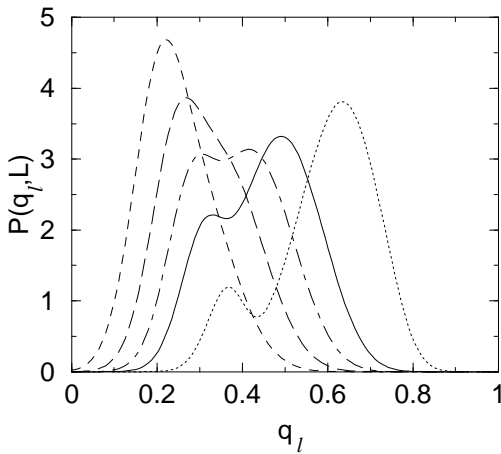


FIG. 6. $P(q_l, L)$ for $T = 0.8T_c, 0.67T_c, 0.56T_c, 0.48T_c, 0.33T_c$ (from left to right), with the system size $L = 4$.

Fig. 7 shows $P(q_l, L)$ for fixed $T = 0.33T_c$ and for different L . One can see that with increasing system size the peaks move closer together, and the weight of the left-hand peak decreases.

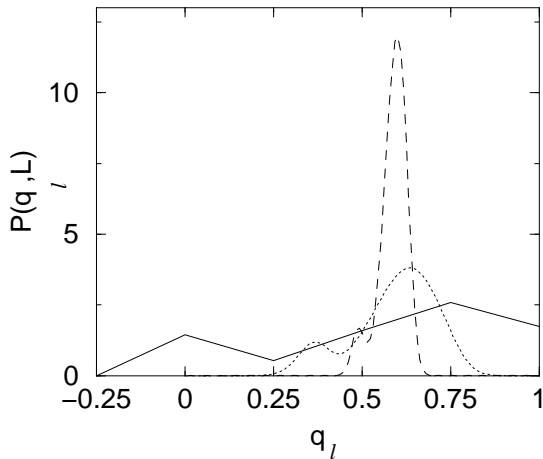


FIG. 7. $P(q_l, L)$ for $L = 2, 4, 8$ (from widest to narrowest curve) and with $T = 0.33T_c$.

These results are similar to what we found in MKA in three dimensions [6], however, in four dimensions the peaks are more pronounced. Monte-Carlo simulations of the four-dimensional Ising spin glass also show two peaks for certain system sizes and temperatures [15]. This feature is attributed by the authors to RSB. However, as it is also present in MKA, there must be a different explanation. The width of the curves shrinks with increasing system size in [15], just as it does in MKA and as is expected from the droplet picture. If the RSB scenario were correct, the width would go to a finite value in the limit $L \rightarrow \infty$.

In the following we present evidence that the left peak corresponds to configurations where one of the two replicas has a domain wall excitation, and the right peak to configurations where one of the two replicas has a droplet

excitation. In MKA, domain wall excitations involve flipping of one side of the system, including one of the two boundary spins of the hierarchical lattice, while droplet excitations involve flipping of a group of spins in the interior. If the sign of the renormalized coupling is positive (negative), the two boundary spins are parallel (antiparallel) in the ground state. By plotting separately the contributions from configurations with and without flipped boundary spins, we can separate domain wall excitations from droplet excitations. Fig. 8 shows the three contributions from configurations where none, one, or both replicas have a domain wall. Clearly, the left peak is due to domain wall excitations, and the right peak to droplet excitations.

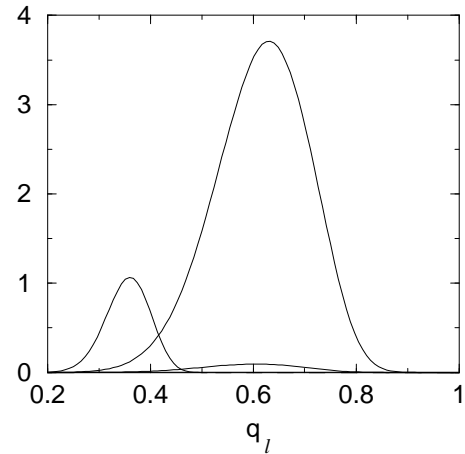


FIG. 8. Contribution of domain wall excitations (left curve) and droplet excitations (right curve) to $P(q_l, L)$, for $L = 4$ and $T = 0.33T_c$. The third, flat curve is due to configurations where both replicas have a domain wall.

Similar curves are obtained for other values of the parameters. We thus have shown that the qualitative differences between droplet and domain wall excitations are sufficient to explain the structure of the link overlap distribution, and no other low-lying excitations like those invoked by RSB are needed.

The weight with which domain-wall excitations occur is in agreement with predictions from the droplet model. The probability of having a domain wall in a system of size L is according to the droplet picture of the order of

$$(T/J)L^{-\theta},$$

which is $\simeq 0.25$ at $T = 0.33T_c$ and $L = 4$, and $\simeq 0.15$ at $T = 0.33T_c$ and $L = 8$. From our simulations, we find that the relative weights of domain walls for these two situations are $\simeq 0.12$ and $\simeq 0.076$, which fits the droplet picture very well if we include a factor 1/2 in the above expression. Domain walls become negligible only when the product $(T/J)L^{-\theta}$ becomes small. In higher dimensions, the critical value of T/J becomes larger, and for a given relative distance from the critical point, the weight

of domain walls therefore also becomes larger. This explains why the effect of domain walls is more visible in 4 dimensions than in 3 dimensions. However, with increasing system size, domain walls should become negligible more rapidly in higher dimensions, due to the larger value of the exponent θ .

VI. CONCLUSIONS

Our results for the Parisi overlap distribution in four dimensions show that there are rather large finite size effects in four dimensions which give rise to phenomena normally attributed to RSB. The system sizes needed to see the beginning of droplet like behavior within the MKA are larger, and the temperatures are lower, than those studied by Monte Carlo simulations. However, at temperatures not too far below those studied in Monte Carlo simulations ($T = 0.5T_c$), the weight of the Parisi overlap distribution function $P(q = 0, L)$ within the MKA appears to decrease, albeit with an effective exponent different from the asymptotic value. Thus, simulations at these temperatures for the Ising spin glass on a cubic lattice might resolve the controversy regarding the nature of the ordered state in short range spin glasses. However, the MKA is a low dimensional approximation and it is possible that the system sizes needed to see asymptotic behavior for a hypercubic lattice in four dimensions are different from what is indicated by the MKA. So, any comparison of the MKA with the Monte Carlo data should be taken with a pinch of salt.

Recently, a modified droplet picture was suggested by Houdayer and Martin [16], and by Bouchaud [17]. Within this picture, excitations on length scales much smaller than the system size are droplet-like, however, there exist large-scale excitations that extend over the entire system and that have a small energy that does not diverge with increasing system size. As we have demonstrated within MKA, the double-peaked curves for the link overlap distribution, can be fully explained in terms of two types of excitations that contribute to the low-temperature behavior, namely domain-wall excitations and droplet excitations. We therefore believe that there is no need to invoke system-wide low-energy excitations that are more relevant than domain walls.

Finally, the whole field of dynamical studies of spin glasses is thought by many [18] to provide a strong reason for believing the RSB picture. A very recent study of spin glass dynamics on the hierarchical lattice [19], on which the MKA is exact, indicates that no ageing occurs at low temperatures in the response function whereas in Monte-Carlo simulations on the Edwards-Anderson model and in spin glass experiments ageing is seen in the response function. We suggest that the ageing behavior found in Monte-Carlo simulations and experiment are in fact often

dominated by critical point effects, and not by droplet effects. Indeed we would expect that if the simulations of Ref. [19] were performed at temperatures closer to the critical temperature then ageing effects would be seen in the response function, since near the critical point of even a ferromagnet such ageing effects occur [20]. The reason why experiments and simulations on the Edwards-Anderson model see ageing in the response function is that they are probing time scales that may be less than the critical time scale, which is given by

$$\tau = \tau_0(\xi/a)^z,$$

with a the lattice constant and τ_0 the characteristic spin-flip time. The dynamical critical exponent $z \simeq 6$ in 3 dimensions [21]. Only for droplet reversals which take place on time scales larger than τ (i.e for reversals of droplets whose linear dimensions exceed ξ) will droplet results for the dynamics be appropriate. However, because of the large values of ξ down to temperatures of at least $0.5T_c$ and the large value of z , τ may be very large in the Monte-Carlo simulations and experiments. Thus if ξ/a is 100, then τ/τ_0 is 10^{12} , which would make droplet like dynamics beyond the reach of a Monte-Carlo simulation. In practice, most data will be in a crossover regime leading to an apparently temperature dependent exponent $z(T)$ (see for example Ref [22]).

ACKNOWLEDGMENTS

We thank A. P. Young for discussions and for encouraging us to write this paper. Part of this work was performed when HB and BD were at the Department of Physics, University of Manchester, supported by EPSRC Grants GR/K79307 and GR/L38578. BD also acknowledges support from the Minerva foundation.

- [1] J.D. Reger, R.N. Bhatt, and A.P. Young, Phys. Rev. Lett. **64**, 1859 (1990).
- [2] E. Marinari, G. Parisi, F. Ricci-Tersenghi, and J.J. Ruiz-Lorenzo in (*Spin Glasses and Random Fields*, ed: A. P. Young), (World Scientific, Singapore, 1997) and references therein.
- [3] M. A. Moore, H. Bokil and B. Drossel, Phys. Rev. Lett. **81**, 4252 (1998).
- [4] H. Bokil, A. J. Bray, B. Drossel, M. A. Moore, Phys. Rev. Lett. **82**, 5174 (1999).
- [5] H. Bokil, A. J. Bray, B. Drossel, M. A. Moore, Phys. Rev. Lett. **82**, 5177 (1999).
- [6] Barbara Drossel, Hemant Bokil, M. A. Moore, and A. J. Bray, European Physical Journal B **13**, 369-375 (2000).
- [7] B.A. Berg and W. Janke, Phys. Rev. Lett. **80**, 4771 (1998).

- [8] M. Palassini and A. P. Young, Phys. Rev. Lett. **83**, 5126 (1999), and unpublished.
- [9] A. J. Bray and M. A. Moore, Phys. Rev. Lett. **58**, 57 (1987).
- [10] E. Marinari and F. Zuliani, cond-mat/9904303.
- [11] A. Hartmann, Phys. Rev. E **60**, 5035 (1999).
- [12] B.W. Southern and A.P. Young, J. Phys. C **10**, 2179 (1977).
- [13] E. Gardner, J. Physique **45**, 1755 (1984).
- [14] R.N. Bhatt and A.P. Young, Phys. Rev. B **37**, 5606 (1988).
- [15] J.C. Ciria, G. Parisi, and F. Ritort, J. Phys. A: Math. Gen. **26**, 6731 (1993).
- [16] J. Houdayer and O.C. Martin, cond-mat/990878.
- [17] J.P. Bouchaud, cond-mat/9910387.
- [18] Silvio Franz, personal communication, (1999).
- [19] F. Ricci-Tersenghi and F. Ritort, cond-mat/9910390.
- [20] C. Godrèche and J. M. Luck, cond-mat 0001264.
- [21] R.E. Blundell, K. Humayan and A.J. Bray, J. Phys. A: Math. Gen. **25**, L733 (1992).
- [22] T. Komori, H. Yoshino and H. Takayama, J. Phys. Soc. Jpn. **68**, 3387 (1999).